Supplement of Atmos. Meas. Tech., 19, 4201–4217, 2026
https://doi.org/10.5194/amt-19-4201-2026-supplement

Atmospheric Measurement Techniques
Open Access
EGU

Supplement of

Design, operation and characterization of a mobile laboratory for hyper-local atmospheric research

Samuel J. Cliff et al.

Correspondence to: Allen H. Goldstein (ahg@berkeley.edu) and Joshua S. Apte (apte@berkeley.edu)

Figure S1 Side on view of the CalMAPLab through the passenger cargo door. On the left is the gas phase rack containing the Aeris CH_4/C_2H_6, Aeris CO/N_2O, 2BTech O_3, CAPS NO_2 and EcoPhysics NO_x and on the right is the Vocus PTR-ToF-MS in the yellow rack. Sample lines can be seen entering through the roof inlet plates and distributed to the different instruments.

Figure S2: View of the CalMAPLab through the rear cargo doors. On the left is the mostly particle phase rack containing the TSI CPC, Magee AE33, Spider Magic, Palas Fidas, DMT PAX and the Licor CO_2 instruments. It also hosts the van server wired into the router and rooftop antennae through the white cables. On the right is the battery electric system with batteries on the bottom and inverters, busbars and fuse boxes above.

Figure S3: Front-on view of the CalMAPLab in its indoor parking space featuring the gas and particle phase inlet lines mounted to an extruded aluminium rail. Also visible are the Airmar WX200 weather station and MetOne pyranometer.

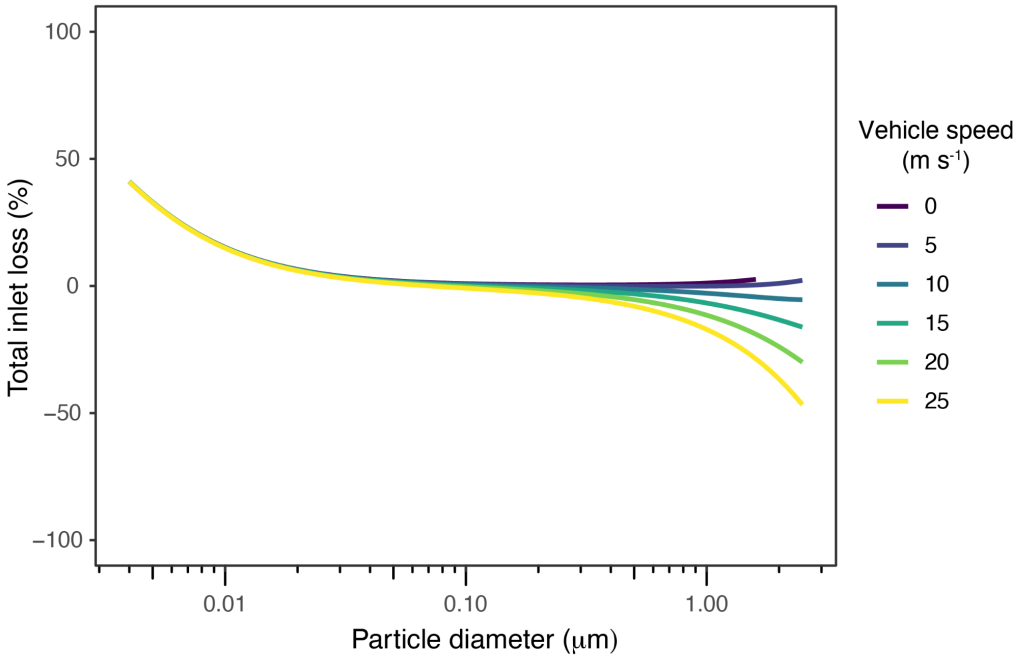

Figure S4: Size disaggregated particle loss calculations for inlet at different driving speeds.

Figure S5: VanDAQ time series dashboard for key measured species by instrument. Individual panels can be configured to show multiple species on different axis (e.g. Aeris instruments). Standard operations display the last 5-minutes of data. Should a measured parameter be out of range (e.g. Aeris CO/N_2O), that instrument flashes red to alert the operator.

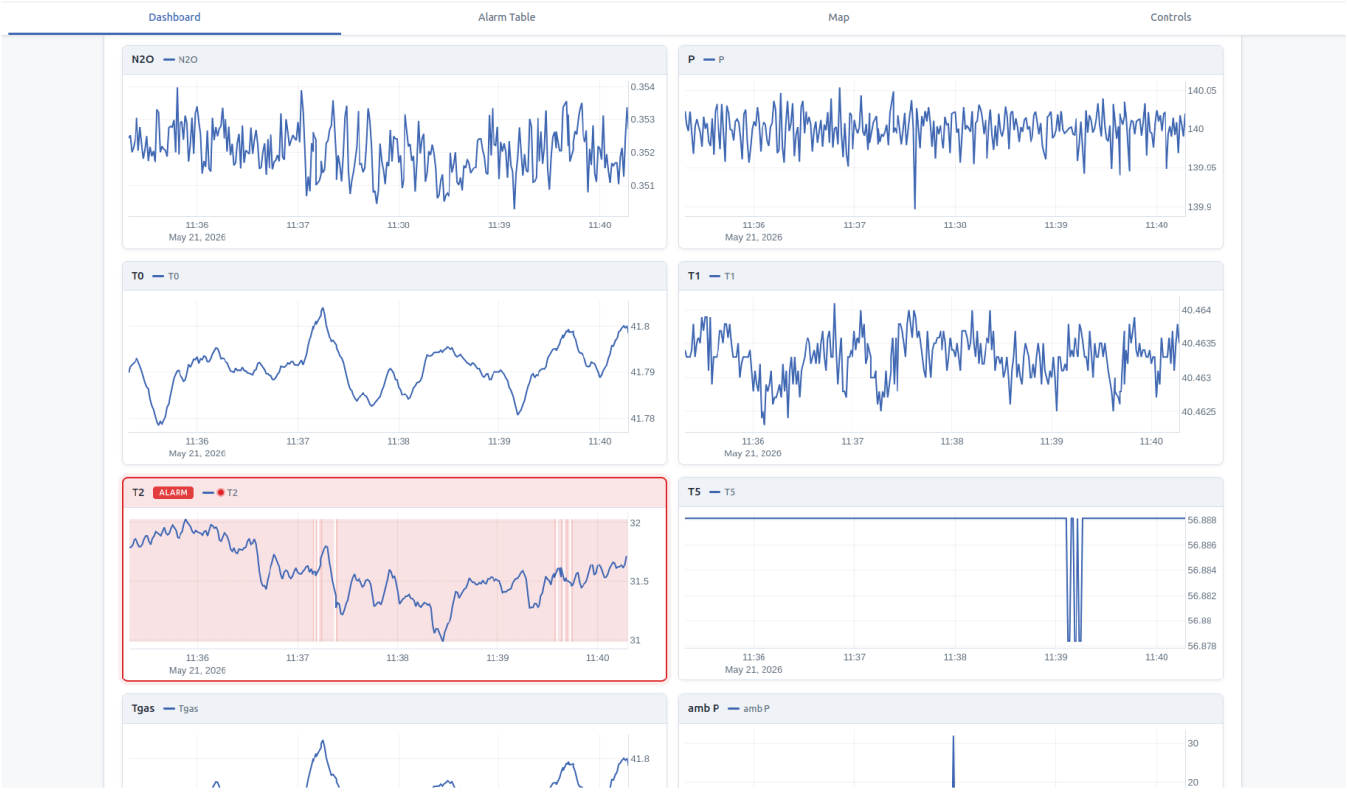

Figure S6: Measured engineering parameters can be studied by clicking on each instrument to open a second set of time series. As with Figure S5, parameter alarms triggered due to a measurement being out of range flash red. The example here is T2 on the Aeris CO/N_2O instrument.

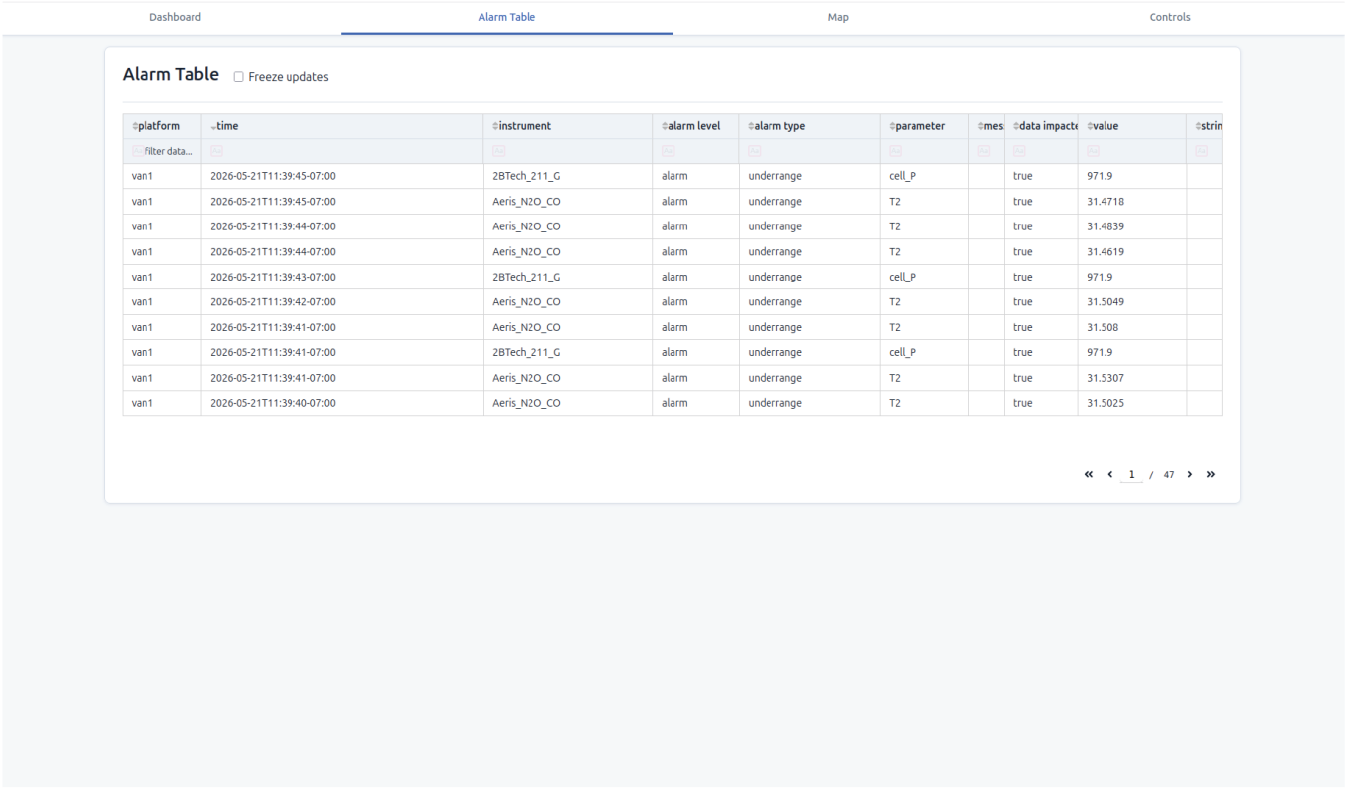

Figure S7: Alarm tables panel within the VanDAQ dashboard. Here, the same Aeris CO/N_2O example as in Figure S5/6 is presented with T2 out of range.

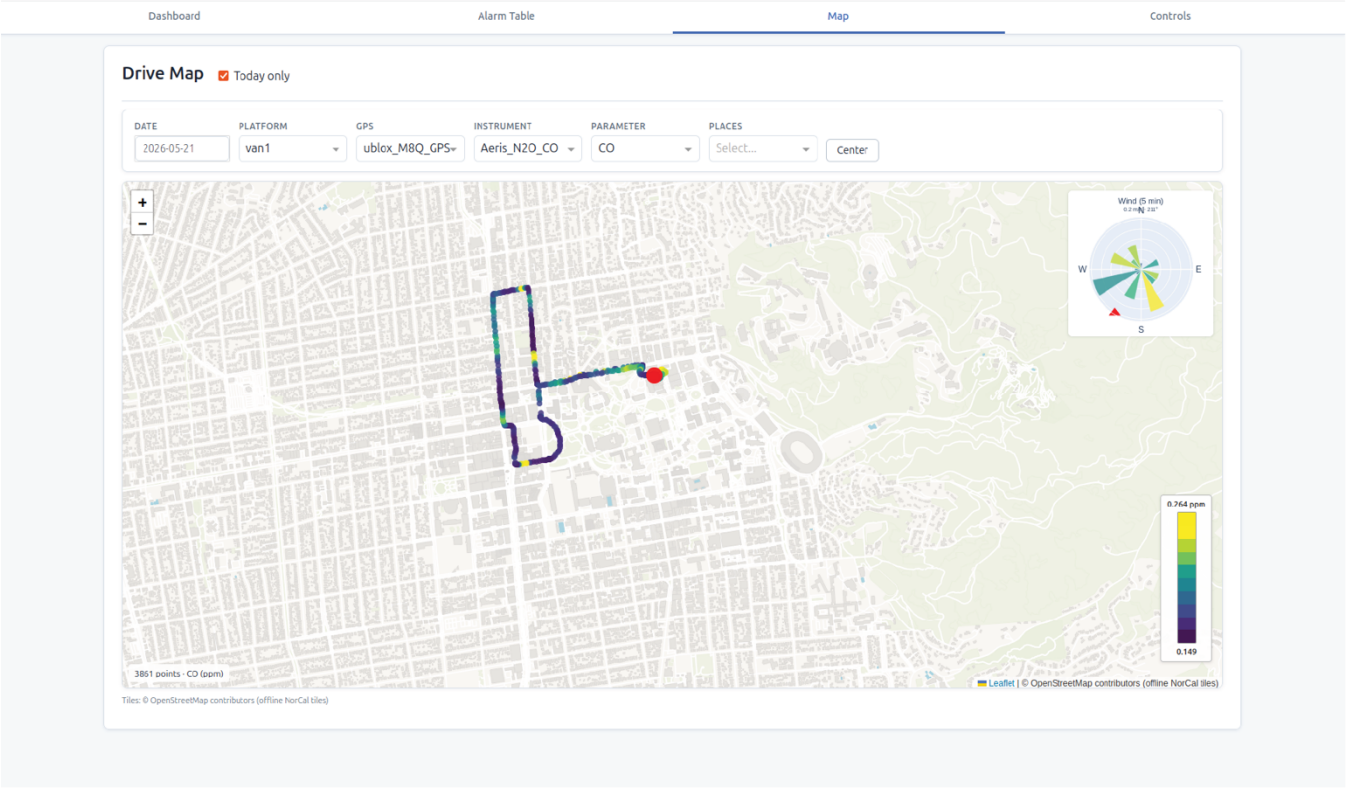

Figure S8: VanDAQ live-updating map of GPS coordinates colored by a choice of instrument parameter values which are toggled in the dropdown menus. Different shape files of polygons or points of interest can be added through the places tab. Historical drive data in the database can be viewed by changing the date field in the calendar dropdown. Also shown is a 5-minute average wind rose from the weather station.

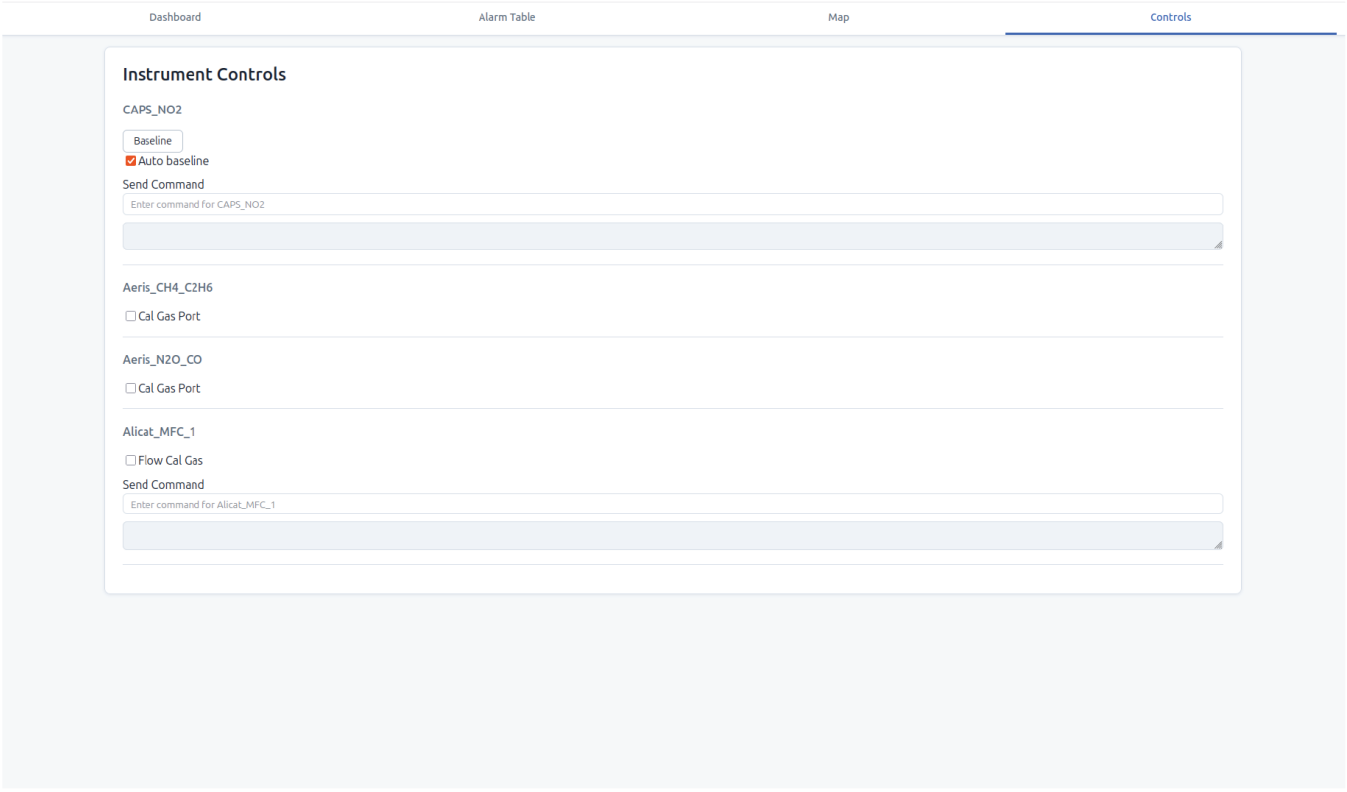

Figure S9: VanDAQ controls tab for triggering valves configured within the system. Here, buttons exist to control the CAPS NO_2 auto baseline, change the Aeris instrument ports, and adjust settings on a mass flow controller.

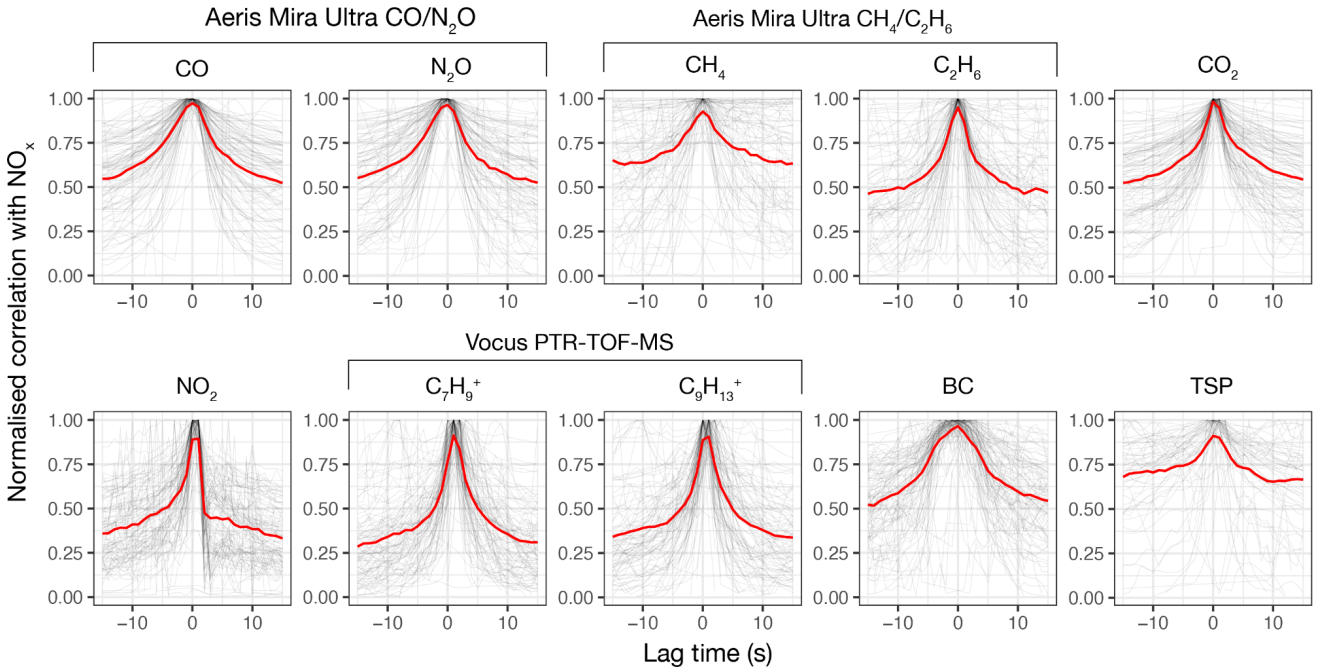

Figure S10: Lag verification from cross correlation statistics of individual drives and measured variables compared to NO_x, where sufficient co-emission in vehicle exhausts enables a lag comparison between all instrumentation excluding the 2BTech 211-G O_3 (no emissions) and $PM_{2.5}$ (slow acquisition rate). Black traces are individual drives and the red trace is the mean average of all drives.

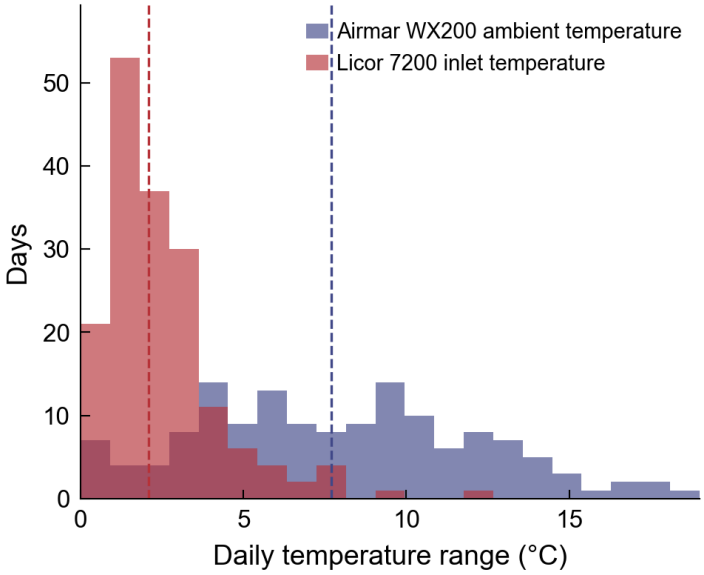

Figure S11: Distributions of temperature range (max-min) for individual drives as measured on the roof with the Airmar WX200 weather station and at the Licor 7200 inlet. The lower magnitude and narrower range of the Licor highlights strong thermal buffering within the sample line relative to ambient temperature.

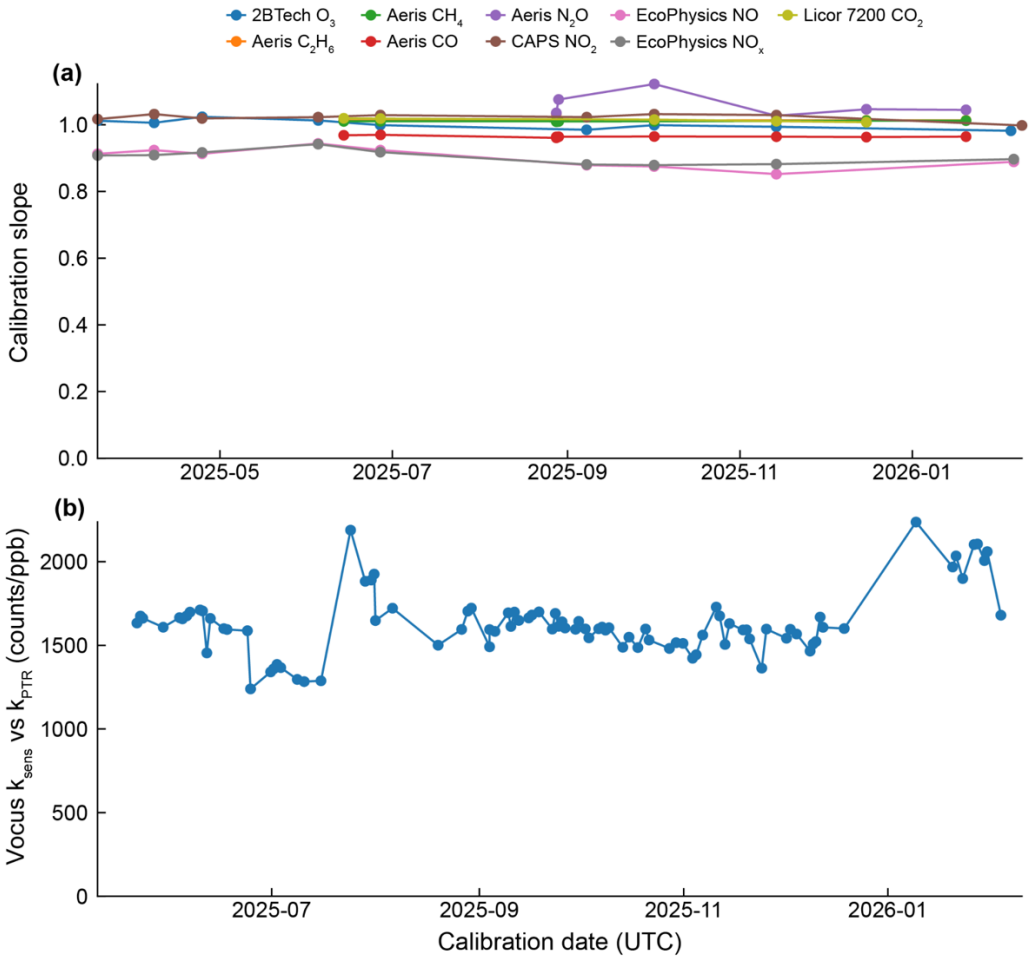

Figure S12: Stability of calibration slopes over ~8 months of operation for a) O_3, CH_4, C_2H_6, N_2O, CO, NO, NO_2, NO_x and CO_2, and b) the Vocus k_{sens} vs k_{PTR}.

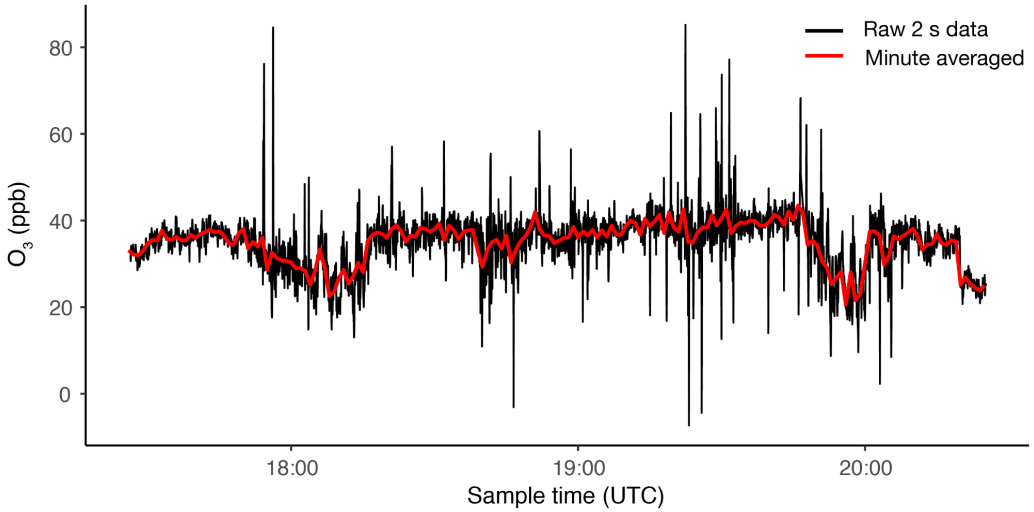

65 **Figure S13:** 2BTech O_3 motion sensitivity for a single drive where averaging data removes the data spikes.

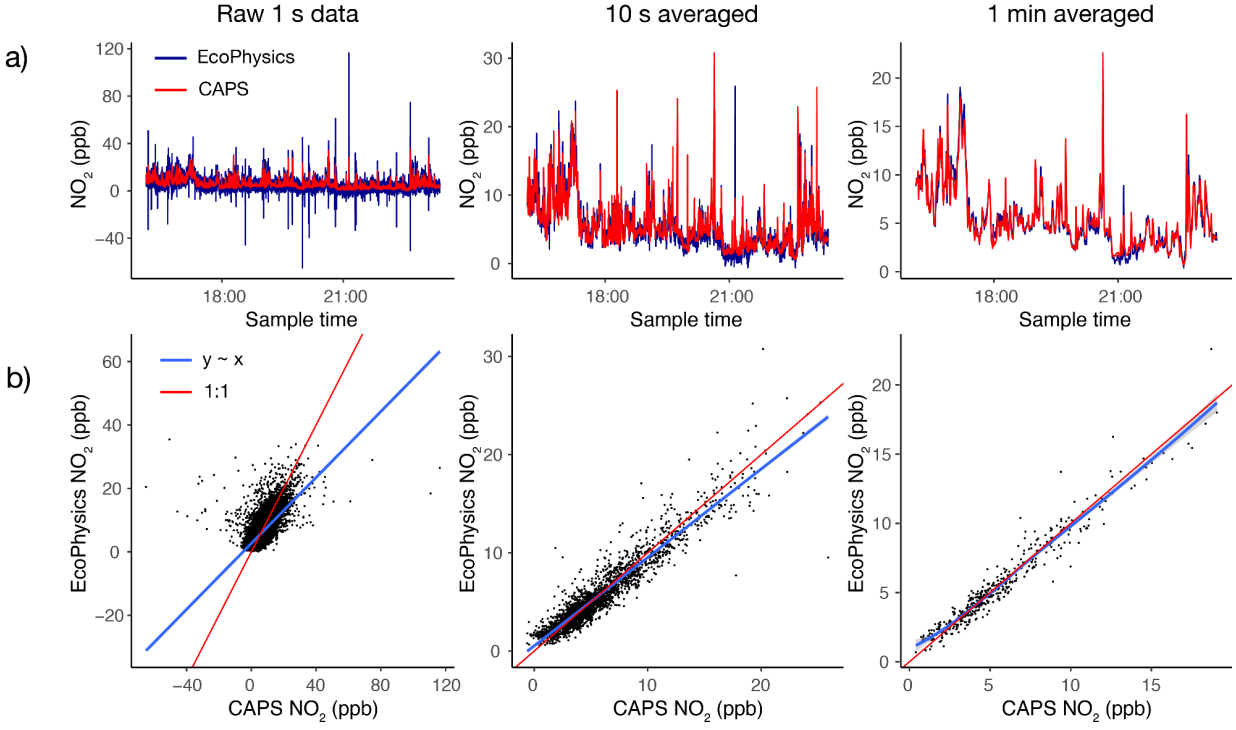

Figure S14: NO_2 comparison between EcoPhysics and Aerodyne CAPS analyser. Data from a single drive at three different aggregation periods: raw 1s, 10s and 1 minute. a) is the drive time series, and b) is a scatter plot of the individual points.

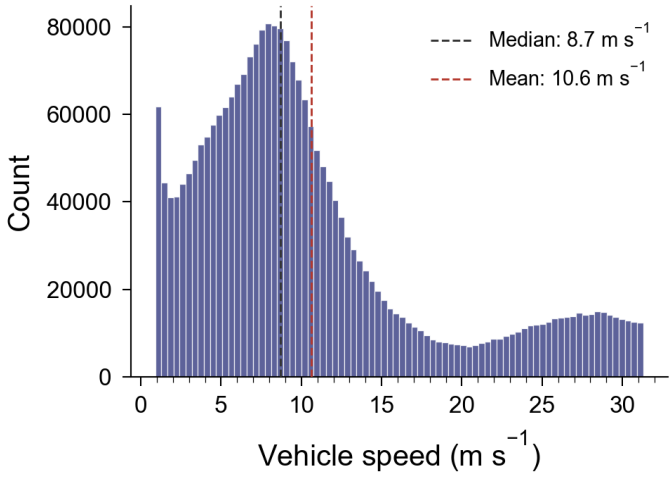

Figure S15: Distribution of mobile vehicle speeds with mean and median statistics indicated as vertical lines.

Table S1: Typical Vocus PTR-ToF-MS operating conditions.

Parameter	**Value setpoint**
Reagent ion flow	15 sccm
IMR pressure	2.5 mbar
IMR temperature	100 C
Electric field gradient	610 V
RF	450 V
Skimmer 1	-10.0 V
Skimmer 2	-17.6 V
BSQ	200 V

Table S2: Typical Spider-MAGIC operating conditions.

Parameter	**Value setpoint**
Sheath flow	900 ccm
Aerosol flow	300 ccm

DP 1	9.6 nm
DP 2	507.6 nm
Charge distribution	Soft X-Ray
HV polarity	+/-
Direction	Both
Bins / dec	40
Diffusional losses correction	TRUE
Multi charge correction	TRUE
Dynamic Z+/Z-	TRUE
Total scan length	29.6 s

Table S3: Parameter precision (1σ) and bias (μ) of the 1 Hz measurement data within in-drive target calibrations across the testing measurement period.

Instrument	Parameter	Precision (1σ, ppb)	Bias (μ, ppb)
Aeris Mira Ultra CO/N_2O	CO	0.63	-1.99
	N_2O	1.09	-0.82
Aeris Mira Ultra CH_4/C_2H_6	CH_4	1.55	18.90
	C_2H_6	0.22	-0.13
Vocus PTR-ToF-MS	$C_2H_5O^+$	0.16	0.14
	$C_2H_7O^+$	0.46	0.17
	$C_3H_4N^+$	0.11	0.05
	$C_3H_7O^+$	0.10	0.08
	$C_4H_7O^+$	0.12	0.00
	$C_4H_9O^+$	0.11	0.06
	$C_5H_9^+$	0.09	0.19
	$C_7H_9^+$	0.11	0.13
	$C_8H_{11}^+$	0.14	0.06
	$C_9H_{13}^+$	0.22	0.00
	$C_{10}H_{17}^+$	0.24	0.03